RSC Advances

ROYAL SOCIETY OF CHEMISTRY

www.rsc.org/advances

Table of Content

A new series of POM-organic hybrids have been developed which shows less genotoxicity compared to the parent polyoxometalate cluster.

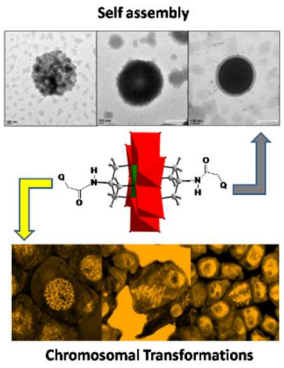

Journal Name

RSCPublishing

COMMUNICATION

Synthesis, Structure, Self-assembly and Genotoxicity Evaluation of a Series of Mn-Anderson Cluster based Polyoxometalate-organic Hybrids†

Cite this: DOI: 10.1039/xoxxoooooox

Received ooth January 2012,
Accepted ooth January 2012

DOI: 10.1039/xoxxoooooox

www.rsc.org/

V. S. V. Satyanarayana,[a‡] Pulikanti Guruprasad Reddy[a‡] and Chullikkattil P. Pradeep[a]*

A new series of class II polyoxometalate-organic hybrids based on Mn-Anderson type polyoxometalate cluster and aromatic organic moieties have been synthesized and characterized through various analytical and spectroscopic techniques including single crystal X-ray analyses in some cases. The genotoxic effects of these covalent hybrids were evaluated by studying their effects on *Allium cepa* cells which revealed their low toxic nature as compared to the parent polyoxometalate cluster.

Polyoxometalates (POMs) are large and significant group of metal-oxygen anionic clusters with discrete structures, which have been extensively studied for their potential applications in catalysis, analytical chemistry, magneto chemistry, materials sciences, medicines and biology.[1] Attachment of organic functionalities onto POM clusters leads to the development of POM-organic hybrids having improved properties and applications. Among the POM-organic hybrids, class II type hybrids in which POMs are covalently bound to organic units are of particular interest because of their stability and possible synergistic interactions between POM and organic components.[2] Therefore, much efforts have been devoted to the development of class II POM hybrids for a variety of applications in recent years.[3-4] Especially, Mn-Anderson cluster based hybrids have resulted in a new class of soft-materials and hybrid polymers.[3] Therefore, the development of new class II POM hybrids based on Mn-Anderson cluster based hybrids targeting new applications is of great importance.

Meanwhile, studies on medicinal and biological properties of POMs have gained momentum in recent years. POM based drugs are projected to have certain advantages over the traditional organic based drugs. Molecular properties of POMs such as their shape, redox potential, acidity and polarity can be easily fine-tuned in order to improve their recognition behaviours towards biomolecules.[1] However, one major problem faced in the development of POM based drugs is the issue of toxicity and accompanying side effects.[5-8] Organic derivatization is widely considered as one of the methods to improve the bio-compatibility of the clusters and hence to minimize their adverse side-effects.[9] Several studies have shown that POM derivatives exhibit biological effects like selective enzyme inhibition, anti-viral (particularly anti-HIV), anti-tumour and anti-bacterial properties[1,5,6,10] but their effect on cell genetics have not yet been explored in detail. Therefore, in the present study we decided to evaluate the genotoxic effects of a series of new POM-organic hybrids derived from Mn-Anderson cluster and various aromatic organic moieties such as naphthalene, quinolone and carabazole derivatives. These organic moieties were selected because of their well-known biological properties including anticancer, antifungal, antibacterial and antiviral properties.[11,12]

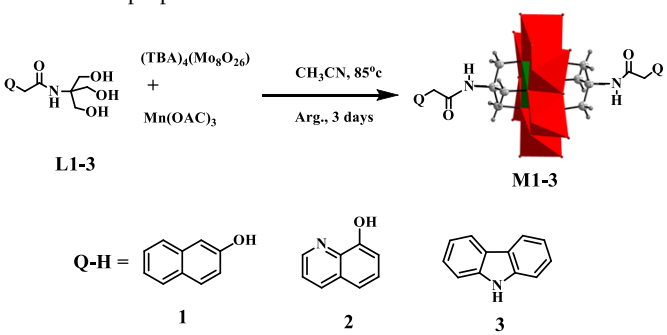

Scheme 1. Synthetic protocol of hybrids **M1-M3**.

The POM–organic hybrids **M1-M3** were synthesized by grafting aromatic organic derivatives **L1-L3** onto Mn-Anderson cluster as sown in Scheme 1. Hybrids **M1-M3** are found to exhibit interesting self-assembly properties in solid state, solutions and in gas phase as revealed by single crystal X-ray analyses, dynamic light scattering (DLS), transmission electron microscopy (TEM) and electrospray ionization mass spectrometry (ESI-MS) analyses. Most importantly, these compounds were tested as model POM-hybrids for their genotoxicity properties. The induction of chromosomal abnormalities in **M1-M3** treated cells were compared with the results of their parent cluster $TBA_3[MnMo_6O_{18}\{(OCH_2)_3C\text{-}NH_2\}_2]$,[3k] (**C1**), (TBA = tetrabutylammonium) treated cells using confocal microscopy. It was found that the hybrids **M1-M3** exhibit less toxic nature compared to the underivatized Mn-Anderson cluster **C1**. The details of these studies are presented in the following sections.

The tris(hydroxymethyl)aminomethane (Tris) derivatives, **L1-L3**, were synthesized by reacting the corresponding esters **E1-E3** (ESI, Scheme S1) with Tris in presence of K_2CO_3 and DMSO at 35 °C for 24 hours. The POM-organic hybrids **M1-M3** were prepared by refluxing **L1-L3** with $TBA_4[Mo_8O_{26}]$ and $Mn(OAC)_3$ in dry acetonitrile under argon atmosphere for 3 days (Scheme 1). The hybrids **M1-M3** are soluble in common organic solvents such as acetonitrile, dimethyl formamide and dimethyl sulfoxide and their structures were determined by FT-IR, ^1H & ^{13}C NMR, ESI-MS and TGA analyses. The molecular structures of hybrids **M1** and **M2** were confirmed by single crystal X-ray analyses as well.

The proton NMR spectra of hybrids **M1-M3** in DMSO-d_6 showed clearly resolved signals that can be assigned to the expected molecular structures unambiguously. The signals exhibited by these compounds in the chemical shift range of 7.20-8.84 ppm correspond to the aromatic protons of the organic moiety as well as the NH proton of the amide functionality. A broad peak appearing at highly down fielded chemical shift region (64-65 ppm)[3c] is characteristic of the Tris-OCH_2 moiety attached to the Mn-Anderson type cluster (see ESI for ^1H and ^{13}C NMR spectra of compounds **M1-M3**).

FT-IR spectra of **M1-M3** were quite similar to each other and were in agreement with the proposed structures. The characteristic vibration bands observed at around 938, 926 and 912 cm^{-1} are assigned to the vibrations of terminal Mo=O units, whereas the bands observed in the range 657-667 cm^{-1} are assigned to the bridging Mo–O–Mo units of Mn-Anderson cluster.[13] The characteristic peaks observed at around 1700 cm^{-1} belong to the C=O group of the amide functionality. The bands between 1024 and 1153 cm^{-1} are assigned to the C–O linkage between the organic moiety and the cluster, confirming successful tethering of the Tris derivatives **L1-L3** onto the Mn-Anderson cluster (see ESI, Figure S1).

ESI-MS analyses of the hybrids **M1-M3** showed similar spectral features. Compounds **M1**, **M2** and **M3** showed three to four groups of peaks in the *m/z* range 1200−2200 having different charges of 3^-, 2^- and 1^-. All the major peaks appearing in the mass spectra of **M1-M3** could be satisfactory assigned to the corresponding parent cluster anion formula with various combinations of counter ions TBA, Na^+ and H^+. Interestingly, some of the peaks appearing in the ESI-MS spectra of these hybrids correspond to dimers of the hybrids. For example, the peaks observed at *m/z* values 1258.09 (3^-) for **M1**, 1259.16 (3^-) for **M2** and 1288.79 (3^-) for **M3** can be assigned to the molecular formulae $TBA_3[MnMo_6O_{18}\{(OCH_2)_3C\text{-}NH\text{-}CO\text{-}C_{11}H_9O\}_2]_2^{3-}$, $TBA_3[MnMo_6O_{18}\{(OCH_2)_3C\text{-}NH\text{-}CO\text{-}C_{10}H_8NO\}_2]_2^{3-}$ and $TBA_3[MnMo_6O_{18}\{(OCH_2)_3C\text{-}NH\text{-}CO\text{-}C_{13}H_{10}N\}_2]_2^{3-}$ respectively (see ESI, Figures S2-S9 and Table S1-S3 for more details). The observation of such dimers in the case of POM-organic hybrids under normal mass spectroscopic conditions is rare in the literature.[3c] Hydrogen bonded aggregates of Dawson cluster derivatives have been reported earlier under cryospray mass spectroscopic conditions.[4d] In the present case, we assume that a combination of weak bonding interactions like the π-π stacking interactions[14] between the aromatic moieties of the hybrid clusters as well as the hydrogen bonding interactions between the cluster and the organic moieties/TBA counterions could be the reason behind the observation of such dimers in the mass spectrum.

The preliminary thermal studies on hybrids **M1-M3** were conducted by using thermogravimetric analyses (TGA). The TGA profiles shown in ESI Figure S10 reveal that in all these cases, weight loss occurs in the temperature range 25-600 °C probably due to the loss of organic moieties of the hybrids. The calculated weight loss corresponding to the loss of three TBA counter-ions and two units of Tris-aromatic moiety attached to the hybrid match very well with the observed weight loss as follows: **M1** = calc. 59.09%, obs. 59.54%; **M2** = cal. 59.14%, obs. 59.96% and **M3** = cal. 59.91%, obs. 60.29%.

Orange coloured single crystals of hybrids **M1,** $TBA_3[MnMo_6O_{18}\{(OCH_2)_3C\text{-}NH\text{-}CO\text{-}C_{11}H_9O\}_2]$, and **M2,** $TBA_3[MnMo_6O_{18}\{(OCH_2)_3C\text{-}NH\text{-}CO\text{-}C_{10}H_8NO\}_2]$, were obtained from their acetonitrile and DMF solutions respectively by slow evaporation method. However, efforts to grow suitable single crystals of **M3** were unsuccessful probably because of its poor crystalline nature. Single crystal X-ray diffraction studies on **M1** and **M2** confirmed the covalent attachment of Tris-aromatic moieties **L1 & L2** respectively onto the Mn-Anderson cluster as expected. The crystal data and structure refinement parameters for **M1** and **M2** are given in Table S4, ESI.

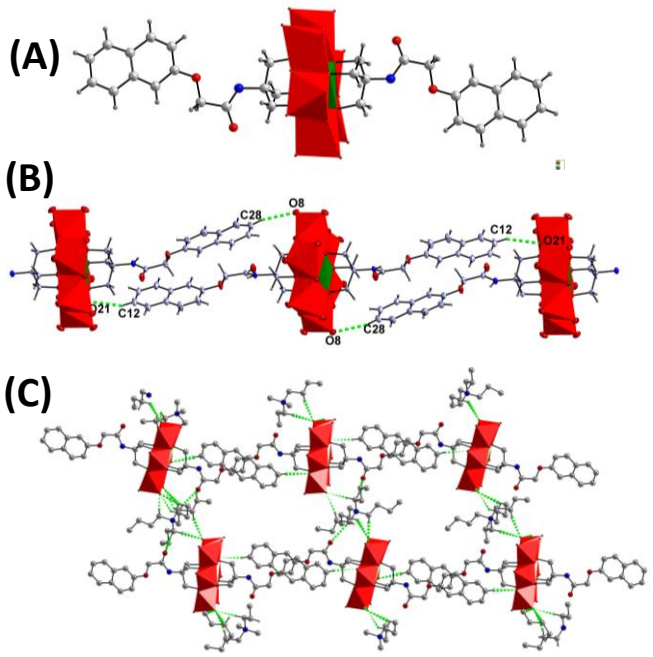

Figure 1. a) Molecular structure of the hybrid cluster in **M1**; **b)** one dimensional chain like polymeric arrangement of hybrid cluster anions of **M1** through H-bonding interactions; **c)** inter-linkage of polymeric 1-D chains through H-bonding interactions with sandwiching TBA counterions leading to 3-D supramolecular framework structure. For clarity, TBA counterions and acetonitrile molecules are omitted except in **c**) where only some of the TBA/TBA parts are shown. Colour code: MoO_6 - red, MnO_6 - green, C - dark grey, H - grey, N - blue, O - red.

The hybrid **M1** crystallized in monoclinic space group $P2_1/c$ with $Z = 4$. The asymmetric unit consists of two half hybrid cluster units, 3 TBA counterions and 5 CH_3CN molecules. The molecular structure of the hybrid cluster unit of **M1** is given in Fig.1(a). In the crystal lattice, the naphthalene carbon C12 of one of the hybrid cluster part present in the asymmetric unit undergo C–H···O hydrogen bonding interactions with the bridging cluster oxygen O21 of the second hybrid cluster part as shown in Fig. 1 (b). Similarly, the naphthalene carbon C28 present on the 2nd hybrid cluster part of the asymmetric unit undergo C–H···O hydrogen bonding interactions with terminal oxygen atoms O8 of the first hybrid cluster part. These interactions lead to the formation of stepped one-dimensional (1-D) chain-like assembly along the *a* axis of the crystal lattice. These 1-D chains are interconnected through additional C–H···O

interactions between the cluster oxygens and sandwiching TBA counterions in a three dimensional (3-D) manner as shown in Fig. 1 (c) leading to the formation of a supramolecular 3-D hydrogen bonded framework structure in the crystal lattice. Solvent molecules occupy the space in the framework structure. The details of the C–H···O hydrogen bonding interactions between TBA counterions and the cluster oxygens are given in ESI, Table S5.

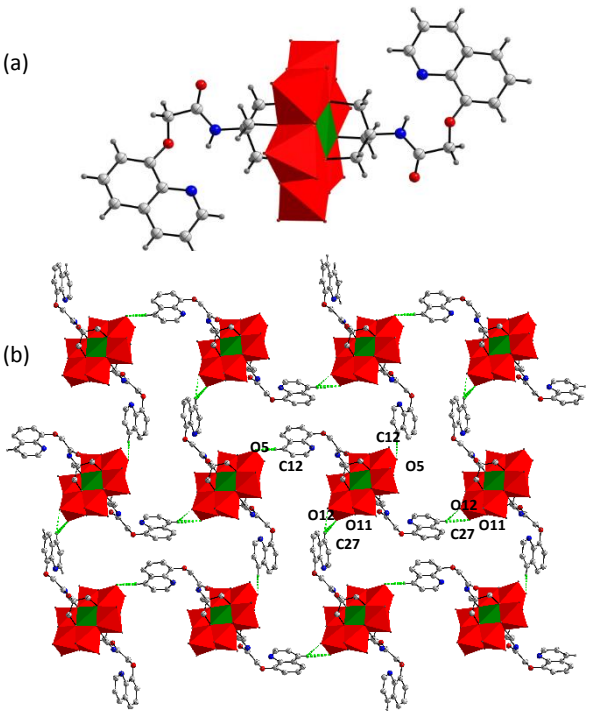

Figure 2. a) Molecular structure of the hybrid cluster in **M2**; **b)** two dimensional polymeric arrangement of hybrid cluster anions of **M2** through H-bonding interactions. Colour code: MoO_6 - red, MnO_6 - green, C - dark grey, H - grey, N - blue, O - red.

Hybrid **M2** crystallized in $P2_1/c$ space group with $Z = 4$. The asymmetric unit contains one hybrid cluster, three TBA counter-ions and two dimethylformamide molecules. The molecular structure of the hybrid cluster is given in Fig. 2 (a). In the crystal lattice, the hybrid cluster units are aligned in a particular chain-like assembly as shown in Fig. 2 (b). The quinoline carbons C12 and C27 of the Tris moiety on either side of the cluster undergo C–H···O hydrogen bonding interactions with POM cluster oxygens (O5 for C12 and O11 & O12 for C27) of adjacent chains on either side. These weak interactions lead to a particular 2-D network assembly of hybrid cluster units in the crystal lattice as shown in Fig 2 (b). Such 2-D arrangement of hybrid cluster units are inter-connected by TBA counter ions sandwiched between cluster units through C–H···O hydrogen bonding interactions. These extensive hydrogen bonding interactions around the cluster hybrid of **M2** in a 3-D manner leads to the formation of a supramolecular hydrogen bonded framework structure in the crystal lattice. The details of these C–H···O interactions are given in Table S6, ESI.

The self-assembly behaviour of hybrids **M1-M3** in solutions were evaluated by using dynamic light scattering (DLS) and transmission electron microscopy (TEM) techniques. The DLS analyses of **M1-M3** performed on their 10^{-3} M solutions in acetonitrile showed average particle sizes in the range: **M1,** 400-600 nm; **M2,** 120-600 nm and **M3,** 60-340 nm (see ESI, Figure S11) probably due to the formation of self-assembled structures in solutions. To confirm the shapes and sizes of these assemblies, the above solutions were subjected to TEM analyses. TEM images show large spherical assemblies of the hybrids with sizes: **M1**, ~400 nm; **M2**, ~500 nm and **M3**, ~300 nm as shown in Fig. 3, which are in agreement with the DLS results. Self-assembly properties of Mn-Anderson cluster based POM-organic hybrids resulting in structures like vesicles, micelles etc. have been reported earlier.[3i,4e,15] Majority of such studies have been conducted in mixed solvent systems. In the formation of such spherical assemblies, weak hydrophobic interactions exerted by the hybrid cluster and the surrounding TBA units are proposed to play significant roles.[15d,e] In the present case, the main reason behind the formation of self-assembled structures of **M1-M3** in MeCN solutions could be the weak bonding interactions between the hybrid clusters and the TBA counterions. This assumption is based on the results of single crystal XRD and ESI-MS studies. The single crystal XRD data of **M1** and **M2** showed that the TBA counterions are sandwiched between adjacent cluster units by engaging in multiple C–H···O hydrogen bonding interactions with the cluster units; thus bringing them closer together. These weak bonding interactions are shown to exist even in gas phase as revealed by the formation of dimers of the hybrids under ESI-MS analytical conditions. Moreover, the grafted aromatic moieties are also capable of promoting self-assembly through π-π stacking interactions.[14] Collective effect of these multiple weak interactions are therefore expected to play constructive roles in the observed self-assembly of these hybrids in solutions.

Preliminary analyses on the self-assembly behaviours of hybrids **M1-M3** under different experimental conditions were also conducted, see ESI page no. 25-31 for details. To understand the role of solute concentration in the observed self-assembly, DLS and TEM analyses were conducted on 10^{-3}, 10^{-4} and 10^{-5} M solutions of the hybrids **M1-M3** in acetonitrile. These studies revealed that the size of the self-assembled structures decreases with decrease in solute concentrations, which is in agreement with similar studies reported earlier,[15b] see ESI Table S7. The self-assembly properties of the hybrids **M1-M3** in different MeCN-H_2O mixed solvent systems were also investigated. These studies showed that an increase in the percentage of water (10-30%) in the solvent mixture leads to increase in the size of the self-assembled structures, see ESI Table S8 and Figures S12 and S13. This is probably because of the fact that the hybrids become less and less soluble with increasing percentage of water in the solution, causing their increased aggregation behaviour. The role of an added salt like $TBAPF_6$ in deciding the self-assembly behaviours of the hybrids **M1-M3** was also tested. The sequential addition of 5, 10, 15 and 20 mg of $TBAPF_6$ into 3 ml 10^{-3} M solution of the hybrids in acetonitrile showed a decrease in the size of the self-assembled structures in solutions, see ESI Table S9 and Figures S14 and S15. These results are in agreement with the results of similar studies reported earlier on Dawson cluster based hybrids in presence of added salts like tetrabutylammonium iodide (TBA·I) and dodecyltrimethylammoniumbromide (DTMA·Br), where the self-assembled structures are found to disintegrate in highly ionic media.[15b]

,

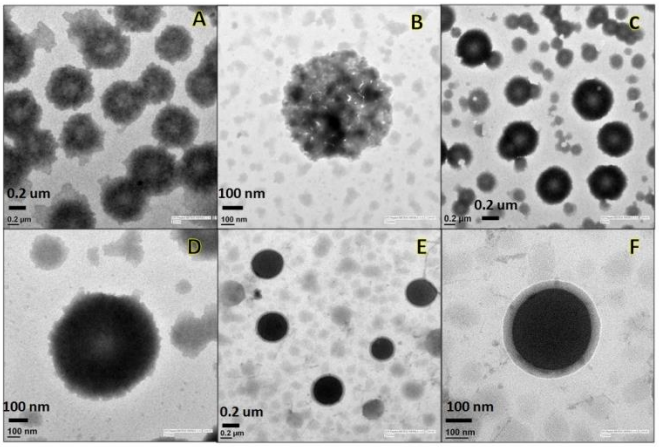

.

Figure **3**. TEM images of hybrids **M1** (A-B), **M2** (C-D) and **M3** (E-F).

The genotoxic effects of hybrids **M1-M3** were screened using *Allium cepa* test. The Allium root chromosomal aberration assay is an established bio-assay recognized by various international agencies as a standard test for the chemical screening of environmental substances.[16] *Allium cepa* test enables the assessment of different genetic endpoints.[17] Among these, chromosomal aberrations have been the most widely used endpoint to detect genotoxic effect of mutagens or potential carcinogens. The mitotic index is another endpoint which has been used as a parameter to assess the toxicity of several agents. Since the target of this analysis, DNA, is common to all organisms, the results of *Allium cepa* test may serve as an indicator of the harmful effects of the toxic material under study towards other biological systems as well.[18]

The mitotic index (MI) and chromosomal aberrations (CA) of *Allium cepa* root meristematic cells treated with varying concentrations of hybrids **M1-M3** were evaluated using standard procedures with slight modifications.[19] As controls, studies have also been conducted on underivatized Tris-Mn-Anderson hybrid $TBA_3[MnMo_6O_{18}\{(OCH_2)_3C\text{-}NH_2\}_2]$, **C1,** as well as on organic moieties, **L1-L3**, to assess their individual genotoxic properties in comparison to the hybrids **M1-M3**. Due to the poor solubility of hybrids in water, distilled water-DMSO mixture was used for these studies as it is a commonly used solvent system for biological studies in the case of water insoluble compounds.[20] These results along with the results of standard positive control (H_2O_2) and negative control (distilled water-DMSO mixture) are given in Table 1.

The mitotic index (MI) is a parameter that estimates the frequency of cellular division. The negative control, distilled water-DMSO mixture, exhibited the highest mitotic index of 13.26% at 250 ppm concentration level (250 ppm of DMSO in water) while the positive control H_2O_2 showed the lowest mitotic index of 1.86% at 250 ppm level. The polyoxometalate control **C1** showed a slightly concentration dependent decrease in the mitotic index values and gave an overall minimum mitotic index of 3.80% at 250 ppm concentration. Compared to **C1**, the hybrids **M1-M3** exhibited better MI values at 250 ppm level (**M1** – 9.20%, **M2** – 9.46% and **M3** – 6.53%) thus showing their less toxic nature compared to **C1**. These values further suggest the dependence of MI values on the organic substituent of the hybrid cluster as well.

Chromosomal aberrations (CA) are characterized by changes in either the chromosomal structure or in the total number of chromosomes. To evaluate CA, several types of aberrations are considered in different phases (prophase, metaphase, anaphase and telophase) of the cell division. Sticky metaphase, chromosome breaks at anaphase, irregular prophase and anaphase bridge are among the prominent chromosomal damages observed in cells treated with the positive control hydrogen peroxide. Distributed pole to pole arrangement of chromosomes at metaphase, telophase laggard, vagrant chromosome and stellate anaphase are the most prominent and repeatable chromosomal damages observed in all the cells treated with the polyoxometalate control **C1**. Chromosomal transformations of *Allium cepa* cells treated with different concentrations of **M1-M3** exhibited minimal aberrations almost similar to those exhibited by negative control (distilled water-DMSO mixture), see ESI Figure S18 for confocal images and further details. As expected, the negative control showed the minimum CA index of 0.66% and the positive control exhibited the maximum CA index of 6.46% at 150 ppm and 250 ppm concentrations respectively. The polyoxometalate control **C1** exhibited a maximum CA index of 3.86% at a concentration of 150 ppm. The hybrids **M1-M3** exhibited the following maximum percentages of CA indices: **M1** = 1.33%, **M2** = 2.00% and **M3** = 2.06 %; the latter two at 250 ppm and the first one at 150 ppm concentrations. These values show that the hybrids **M1-M3** show low CA indices in comparison to those exhibited by the polyoxometalate control **C1**. Meanwhile, the **L1-L3** controls did not show any considerable genotoxic effects as their mitotic and CA indices were almost comparable to those of the negative control; see ESI Fig. S18 (E4-H6) and Table S10 for more details. It can be noted that the hybrids **M1** and **M2** are slightly less toxic than **M3**. One of the reasons for this could be the larger ring size of the organic moiety in **M3** compared to those in **M1** and **M2** as the ring size is shown to play crucial roles in determining the genotoxic nature of certain organic compounds.[21]

The above results demonstrate that the hybrid compounds **M1-M3** are having less genotoxic effects compared to the underivatized parent cluster Tris-Mn-Anderson$TBA_3[MnMo_6O_{18}\{(OCH_2)_3C\text{-}NH_2\}_2]$. Clearly, more studies are required to understand the exact roles of organic groups attached to the cluster hybrids in deciding their less toxic nature.

Conclusions

A new series of class II POM-organic hybrids based on Mn-Anderson cluster and aromatic organic moieties such as naphthalene, quinoline and carbazole derivatives have been synthesized and characterized. Single crystal XRD, DLS, TEM and ESI-MS analyses revealed interesting self-assembly features of these hybrids in solid state, solutions and in gas phase. Most importantly, these hybrids were tested for their genotoxic effects in comparison to the parent underivatized POM cluster using *Allium cepa* test and by evaluating certain genetic endpoints like mitotic index and chromosomal aberrations. Confocal microscopic studies on the *Allium cepa* meristematic cells treated with organically grafted POM-hybrids **M1-M3** and the underivatized parent cluster **C1** revealed the less toxic nature of the organically grafted hybrids in comparison to the underivatized cluster.

Table 1. Mitotic indices and chromosomal aberration indices observed in *Allium cepa* meristematic root tip cells exposed to different concentrations of hybrids **M1-M3** and various controls for 4 hours.

Treatment	Concentration (ppm)	No. of dividing cells	Mitotic Index MI (%)	No. of damaged cells	Chromosomal Aberration index CA (%)
Negative control	50	235	15.66± 2.51	9	0.60 ± 1.00
	150	209	13.93± 3.51	10	0.66 ± 1.52
	250	199	13.26± 3.05	9	0.60 ± 0.57
Positive control	250	28	1.86±2.08	97	6.46 ± 4.51
C1	50	80	5.33±4.04	44	2.93 ± 3.05
	150	72	4.80± 4.16	58	3.86 ± 4.04
	250	57	3.80± 3.78	56	3.73 ± 3.05
M1	50	162	10.80± 4.58	15	1.00 ± 1.52
	150	152	10.13± 3.51	20	1.33 ± 1.00
	250	138	9.20± 3.00	19	1.26 ± 1.52
M2	50	154	10.26±6.24	21	1.40 ± 2.00
	150	174	11.60± 2.51	19	1.26 ± 1.52
	250	142	9.46± 4.58	30	2.00 ± 2.08
M3	50	160	10.66± 5.50	20	1.33 ± 1.73
	150	149	9.93± 4.51	25	1.66 ± 1.00
	250	98	6.53± 4.16	31	2.06 ± 2.00

Mitotic and aberration indices were calculated as: (number of dividing cells or damaged cells / total number of cells observed) × 100.

Acknowledgment

CPP thanks DST New Delhi, for funds under the fast track scheme (Grant No. SR/FT/CS-58/2011) and IIT Mandi for infrastructural facilities as well as financial support through Seed Grant.

Notes and references

[a]: *School of Basic Sciences, Indian Institute of Technology Mandi, Mandi – 175001, Himachal Pradesh, India E-mail: pradeep@iitmandi.ac.in; Fax: (+91)1905 267 009.*

‡: *Both the authors have contributed equally to this work.*

†: Electronic supplementary information (ESI) available: Experimental procedures, characterization data including ^{1}H, ^{13}C NMR, Mass spectra, Single XRD, TGA, TEM and confocal cell images.

1. (a) *Polyoxometalate Chemistry from Topology via Self-Assembly to Applications*, ed. M. T. Pope and A. Müller, Kluwer Academic Publishers, Dordrecht, Netherlands, 2001; (b) C. L. Hill, *Chem. Rev.*, 1998, **98**, 1-2; (c) D.-L. Long, R. Tsunashima and L. Cronin, *Angew. Chem. Int. Ed.*, 2010, **49**, 1736-1758.
2. (a) A. Dolbecq, E. Dumas, C. R. Mayer and P. Mialane, *Chem. Rev.*, 2010, **110,** 6009 – 6048; (b) A. Proust, R. Thouvenot and P. Gouzerh, *Chem. Commun*., 2008, 1837-1852; (c) M.-P. Santoni, G. S. Hanan and B. Hasenknopf, *Coord. Chem. Rev.*, 2014, **281**, 64–85; (d) Y.-F. Song and R.Tsunashima, *Chem. Soc. Rev.*, 2012, **41**, 7384-7402; (e) A. Proust, B. Matt, R. Villanneau, G. Guillemot, P. Gouzerh and G. Izzet, *Chem. Soc. Rev.*, 2012, **41**, 7605–7622; (f) A. Dolbecq, P. Mialane, F. Sécheresse, B. Keita and L. Nadjo, *Chem. Commun.*, 2012, **48**, 8299-8316.
3. (a) B. Hasenknopf, R. Delmont, P. Herson and P. Gouzerh, *Eur. J. Inorg. Chem.*, 2002, 1081-1087; (b) C. Allain, S. Favette, L. M. Chamoreau, J. Vaissermann, L. Ruhlmann and B. Hasenknopf, *Eur. J. Inorg. Chem.*, 2008, 3433–3441; (c) C. Yvon, A. Macdonell, S. Buchwald, A. J. Surman, N. Follet, J. Alex, D.-L. Long and L. Cronin, *Chem. Sci.*, 2013, **4**, 3810–3817; (d) Z. He, B. Li, H. Ai, H. Li and L. Wu, *Chem. Commun.*, 2013, **49**, 8039-8041; (e) Y.-F. Song, D.-L. Long and L. Cronin, *Angew. Chem. Int. Ed*., 2007, **46**, 3900-3904; (f) U. Tong, W. Chen, C. Ritchie, X. Wang and Y.-F. Song, *Chem. Eur. J.*, 2014, **20**, 1500–1504; (g) S. Favette, B. Hasenknopf, J. Vaissermann, P. Gouzerh and C. Roux, *Chem. Commun.*, 2003, 2664-2665; (h) B. Hu, C. Wang, J. Wang, J. Gao, K. Wang, J. Wu, G. Zhang, W. Cheng, B. Venkateswarlu, M. Wang, P. S. Lee and Q. Zhang, *Chem. Sci.*, 2014, **5**, 3404-3408; (i) J. Zhang, Y.-F. Song, L. Cronin and L. Tianbo, *Chem. Eur. J.*, 2010, **16**, 11320 – 11324; (j) Y.-F. Song, N. McMillan, D.-L. Long, S. Kane, J. Malm, M. O.Riehle, C. P. Pradeep, N. Gadegaard and L. Cronin, *J. Am. Chem. Soc.*, 2009, **131**, 1340-1341; (K) P. R. Marcoux, B. Hasenknopf, J. Vaissermann and P. Gouzerh, *Eur. J. Inorg. Chem.*, 2003, 2406-2412; (l) V. Kalyani, V. S. V. Satyanarayana, A. S. Sarkar, A. Kumar, S. K. Pal, S. Ghosh, K. E. Gonsalves and C. P. Pradeep, *RSC Adv.*, 2015, **5**, 36727-36731; (m) A. Macdonell, N. A. B. Johnson, A. J. Surman and L. Cronin, *J. Am. Chem. Soc.*, 2015, **137**, 5662-5665.
4. (a) Y. Hou and C. L. Hill, *J. Am. Chem. Soc.*,1993, **115**, 11823-11830; (b) Y. Wei, B. Xu, C. L. Barnes and Z. Peng, *J. Am. Chem. Soc.*, 2001, **123**, 4083-4084; (c) H. Zheng, G. R. Newkome and C. L. Hill, *Angew. Chem. Int. Ed.*, 2000, **39**, 1771-1774; (d) C. P. Pradeep, D.-L. Long, G. N. Newton, Y.-F. Song and L. Cronin, *Angew. Chem. Int. Ed.*, 2008, **47**, 4388-4391; (e) C. P. Pradeep, M. F. Misdrahi, F.-Y. Li, J. Zhang, L. Xu, D.-L. Long, T. Liu and L. Cronin, *Angew. Chem. Int. Ed.*, 2009, **48**, 8309-8313; (f) C. P. Pradeep, F.-Y. Li, C. Lydon, H. N. Miras, D.-L. Long, L. Xu and L. Cronin, *Chem. Eur. J.*, 2011, **17**, 7472-7479; (g) V. Kalyani, V. S. V. Satyanarayana, V. Singh, C. P. Pradeep, S. Ghosh, S. K. Sharma and K. E. Gonsalves, *Chem. Eur. J.*, 2015, **21**, 2250-2258; (h) P.G. Reddy, V.S.V. Satyanarayana , V. Dubey, A. R. Ghosh and C.P. Pradeep, *Inorg. Chem. Comm.*, 2015, **56**, 65–68.
5. T. Yamase, *J. Mater. Chem.*, 2005, **15**, 4773–4782.
6. B. Hasenknopf, *Front. Biosci.*, 2005, **10**, 275-287.
7. H. U. V. Gerth, A. Rompel, B. Krebs, J. Boos and C. Lanvers-Kaminsky, *Anticancer Drugs*., 2005, **16**, 101-106.

8. (a) W. Rozenbaum, D. Dormont, B. Spire, E. Vilmer, M. Gentilini, C. Griscelli, L. Montagnier, F. Barre-Sinoussi and J. C. Chermann, *Lancet.*, 1985, **325**, 450-451; (b) B. Moskovitz, *Antimicrob. Agents. Chemother.*, 1988, **32**, 1300-1303.
9. J. T. Rhule, C. L. Hill, D. A. Judd and R. F. Schinazi, *Chem. Rev.*, 1998, **98**, 327-357.
10. C. L. Hill, M. S. Weeks and R. F. Schinazi, *J. Med. Chem.*, 1990, **33**, 2767–2772; (b) J. Wang, Y. Liu, K. Xu, Y. Qi, J. Zhong, K. Zhang, J. Li, E. Wang, Z. Wu and Z. Kang, *ACS Appl. Mater. Interfaces.*, 2014, **6**, 9785−9789; (c) F. Pu, E. Wang, H. Jiang and J. Ren, *Mol. BioSyst.*, 2013, **9**, 113-120; (d) L. Wang, K. Yu, B. Bin Zhou, Z.-H. Su, S. Gao, L.-L. Chua and J.-R. Liu, *Dalton Trans.*, 2014, **43**, 6070; (e) H. K. Daima, P. R. Selvakannan, A. E. Kandjani, R. Shukla, S. K. Bhargava and V. Bansal, *Nanoscale*, 2014, **6**, 758–765; (f) M. B. Stuckart, L. F. P. Garza, B. Gautam, G. A. Espinoza, N. V. Izarova, A. Banerjee, B. S. Bassil, M. S. Ullrich, H. J. Breunig, C. Silvestru and U.Kortz, *Inorg. Chem.*, 2012, **51**, 12015−12022; (g) Y. Zhang, J. Q. Shen, L.-H. Zheng, Z.-M. Zhang, Y.-X. Li and E.-B. Wang, *Cryst. Growth Des.*, 2014, **14**, 110−116; (h) D. Zhang, Z. Liang, S. Xie, P. Ma, C. Zhang, J. Wang and J. Niu, *Inorg. Chem.*, 2014, **53**, 9917−9922.
11. (a) W. Kitagawa and T. Tamura, *J. Antibiot.*, 2008, **61**, 680–682; (b) M. A. Fakhfakh, A. Fournet, E. Prina, J.-F. Mouscadet, X. Franck, R. Hocquemiller and B. Figadère, *Bioorg. Med. Chem.*, 2003, **11**, 5013–5023; (c) D. J. Sheehan, C. A. Hitchcock and C. M. Sibley, *Clin. Microbiol. Rev.*, 1999, **12**, 40–79; (d) P. Furet, C. Batzl, A. Bhatnagar, E. Francotte, G. Rihs and M. Lang, *J. Med. Chem.*, 1993, **36**, 1393-1400; (e) A. W. Schmidt, K. R. Reddy and H.-J. Knölker, *Chem. Rev.*, 2012, **112**, 3193−3328.
12. (a) R. S. Upadhayaya, J. K. Vandavasi, R. A. Kardile, S. V. Lahore, S. S. Dixit, H. S. Deokar, P. D. Shinde, M. P. Samah and J. Chattopadhyaya, *Eur. J. Med. Chem.*, 2010, **45**, 1854-1867; (b) A. Milelli, V. Tumiatti, M. Micco, M. Rosini, G. Zuccari, L. Raffaghello, G. Bianchi, V. Pistoia, J. F. Díaz, B. Pera, C. Trigili, I. Barasoain, C. Musetti, M. Toniolo, C. Sissi, S. Alcaro, F. Moraca, M. Zini, C. Stefanelli and A. Minarini, *Eur. J. Med. Chem.*, 2012, **57**, 417-428.
13. (*a*) K. Nomiya, T. Takahashi, T. Shirai and M. Miwa, *Polyhedron*, 1987, **6**, 213–218; (*b*) J. Zhang, Y. Huang, J. Zhang, S. She, J. Hao and Y. Wei, *Dalton Trans.*, 2014, **43**, 2722–2725.
14. J. Gao, X. Liu, Y. Liu, L. Yu, Y. Feng, H. Chen, Y. Li, G. Rakesh, C. H. A. Huan, T. C. Sum, Y. Zhao and Q. Zhang, *Dalton Trans.*, 2012, **41**, 12185-12191.
15. (a) J. Zhang, Y.-F. Song, L. Cronin and T. Liu, *J. Am. Chem. Soc.*, 2008, **130**, 14408–14409; (b) P. Yin, C. P. Pradeep, B. Zhang, F.-Y. Li, C. Lydon, M. H. Rosnes, D. Li , E. Bitterlich, L. Xu, L. Cronin and T. Liu, *Chem. Eur. J.*, 2012, **18**, 8157–8162; (c) M. F. Misdrahi, M. Wang, C. P. Pradeep, F.-Y. Li, C. Lydon, L. Xu, L. Cronin and T. Liu, *Langmuir.*, 2011, **27**, 9193–9202; (d) B. Zhang, C. P. Pradeep, L. Cronin and T. Liu, *Chem. Commun.*, 2015, **51**, 8630-8633; (e) C.-G. Lin, W. Chen and Y.-F. Song, *Eur. J. Inorg. Chem.*, 2014, 3401–3405; (f) D. Li, J. Song, P. Yin, S. Simotwo, A. J. Bassler, Y. Y. Aung, J. E. Roberts, K. I. Hardcastle, C. L. Hill and T. Liu, *J. Am. Chem. Soc.*, 2011, **133**, 14010–14016.
16. G. L. Cabrera and D. M. G. Rodriguez, *Mutat. Res.*, 1999, **426**, 211-214.
17. D. M. Leme and M. A. Marin-Morales, *Mutat. Res.*, 2009, **682**, 71-81.
18. (a) M.B. Joray, M. L. González, S. M. Palacios and M. C. Carpinella, *J. Agric. Food Chem.*, 2011, **59**, 11534–11542; (b) C. L. Potter, J. A. Glaser, L. W. Chang, J. R. Meier, M. A. Dosani and R. F. Herrmann, *Environ. Sci. Technol.*,1999, **33**, 1717-1725; (c) N. I. V. Moreno, I. C. Zampini, R. M. Ordonez, G. S. Jaime, M. A. Vattuone and M. I. Isla, *J. Agric. Food Chem.*, 2005, **53**, 8957-8962; (d) M. Kumari, A. Mukherjee and N. Chandrasekaran, *Sci. Total Environ.*, 2009, **407**, 5243–5246; (e) P. N. Saxena, S. K. Gupta and R. C. Murthy, *Pest. Biochem. and Physio.*, 2010, **96**, 93–100; (f) K. P. Mohammed, A. Aarey, S. Tamkeen and P. Jahan, *Mutat. Res.*, 2015, **777**, 29–32.
19.(a) J. Rank and M.H. Nielsen, *Hereditas*, 1993, **118**, 49-53; (b) A. S. A. Prasad, V.S.V. Satyanarayana and K. V. B. Rao, *J. Hazard. Mater.*, 2013, **262**, 674– 684.
20. (a) Y. Liu, M. Kong, Q. Zhang, Z. Zhang, H. Zhou, S. Zhang, S. Li, J. Wu, and Y. Tian, *J. Mater. Chem. B*, 2014, **2**, 5430–5440; (b) M. Wu, X.-M. Xia, C. Cui, P. Yu, Y. Zhang, L. Liu, R.-X. Zhuo and S.-W. Huang, *J. Mater. Chem. B*, 2013, **1**, 1687–1695; (c) M. Casolaro, R. Cini, B. D. Bello, M. Ferrali and E. Maellaro, *Biomacromolecules*, 2009, **10**, 944-949; (d) W. Zhang, K. Patel, A. Schexnider, S. Banu and A. D. Radadia, *ACS NANO*, 2014, **2**, 1419-1428.
21. (a) S. Zheng, L. Laraia, C. J. O' Connor, D. Sorrell, Y. S. Tan, Z. Xu, A. R. Venkitaraman, W. Wu and D. R. Spring, *Org. Biomol. Chem.*, 2012, **10**, 2590-2593.

